ADIABATIC FORMATION AND PROPERTIES OF A QUASI-EQUILIBRIUM BEAM DISTRIBUTION MATCHED TO A PERIODIC FOCUSING LATTICE*

Mikhail Dorf, Ronald C. Davidson, Edward Startsev and Hong Qin
Plasma Physics Laboratory, Princeton University, Princeton, New Jersey, USA 08543

Abstract

This paper reports on recent advances in the development of a numerical scheme for describing the quiescent loading of a quasi-equilibrium beam distribution matched to a periodic focusing lattice [1]. The scheme allows for matched-beam distribution formation by means of the adiabatic turn-on of the oscillating focusing field, and it is examined here for the cases of alternating-gradient quadrupole and periodic solenoidal lattices. Furthermore, various distributions are considered for the initial beam equilibrium. The self-similar evolution of the matched-beam density profile is observed for arbitrary choice of initial distribution function and lattice type. The numerical simulations are performed using the WARP particle-in-cell code.

INTRODUCTION

Periodic-focusing accelerators and transport systems have a wide range of applications ranging from basic scientific research to industrial applications [2]. It is therefore important to develop an improved theoretical understanding of intense beam transport, stability, and equilibrium properties. However, the effects of the intense self-fields produced by the beam space-charge introduce a significant challenge for analytical studies, and the only known distribution function that provides an exact beam equilibrium in an periodic-focusing lattice is the Kapchinskij-Vladimirskij (KV) distribution [2]. This distribution, however, is unstable at sufficiently high beam intensities, and therefore approximate analytical analysis or numerical models have to be developed to describe other (stable) intense beam quasi-equilibrium solutions.

Recently, a numerical approach for describing the quiescent formation of a quasi-equilibrium beam distribution matched to an alternating-gradient quadrupole lattice by means of adiabatic turn-on of the oscillating focusing field has been proposed in [1]. In this approach, an equilibrium beam distribution is first loaded into the equivalent smooth-focusing uniform channel [2]; then the oscillating feature of the lattice is adiabatically turned-on, and is accompanied by a corresponding decrease in the uniform focusing component. It was demonstrated that the method allows for the quiescent formation of a quasi-equilibrium beam distribution matched to a quadrupole lattice for a broad range of beam intensities and vacuum phase advances describing the strength of the oscillating focusing field. Furthermore, properties of the quasi-equilibrium matched-beam distribution have been investigated and compared to the predictions of analytical theory that applies Hamiltonian averaging techniques to the nonlinear Vlasov-Maxwell equations [2], assuming sufficiently small vacuum phase advance, σ_v. In particular, correct to order ε^3, where $\varepsilon \equiv \sigma_v/2\pi$, the theory predicts the self-similar evolution of the beam density profile. The evolution of the quasi-equilibrium beam density profile obtained in the numerical simulations making use of the adiabatic formation scheme has been investigated. The self-similarity feature was preserved to good accuracy for $\sigma_v < 66^0$, and for a wide range of beam intensity ranging from an emittance-dominated beam with $\sigma/\sigma_v \approx 0.26$, to a space-charge-dominated beam with $\sigma/\sigma_v \approx 0.91$. Here, σ denotes the depressed phase advance. Furthermore, it was shown that for higher values of vacuum phase advance (for instance, $\sigma_v = 87.5^0$) the self-similarity feature becomes less accurate, which demonstrates the validity limits of the theory.

In this paper, we continue developing this method for adiabatic formation of a matched-beam quasi-equilibrium, and generalize it to the case of a periodic focusing solenoidal lattice. Furthermore, other initial smooth-focusing equilibrium distributions, namely a thermal equilibrium and a waterbag equilibrium, are considered.

MODEL DESCRIPTION

In this section, following [1], we summarize the method for adiabatic formation of a quasi-equilibrium beam distribution matched to an alternating-gradient quadrupole lattice, and generalize it to the case of a periodic solenoidal focusing lattice. The method works as follows. First, the oscillating focusing field of the lattice is replaced with the smooth-focusing force, and an equilibrium beam distribution is loaded into a uniform focusing channel. Then the oscillating focusing field is adiabatically turned on as the amplitude of the uniform component is adjusted to maintain the average (smooth-focusing) effects of the total focusing field fixed. For the case of a quadrupole lattice, the *total* focusing force acting on the beam particles is specified by

$$F_q = \left[V^2(s) - 1\right]\kappa_{sf}^q\left(x\mathbf{e}_x + y\mathbf{e}_y\right) - V(s)\,\kappa_q(s)\left(x\mathbf{e}_x - y\mathbf{e}_y\right), \quad (1)$$

where $V(s)$ is a function describing the transition of the applied lattice force and varying from zero to unity, $\kappa_q(s)$ is the quadrupole lattice coupling coefficient, and κ_{sf}^q is the corresponding smooth-focusing value. For the choice of the quadrupole lattice model shown in Fig. 1 it is

*Research supported by the U.S. Department of Energy.

straightforward to demonstrate to leading order that $\kappa_{sf}^{q} = (1/16)\eta_q^2 \hat{\kappa}_q^2 S^2 (1 - 2\eta_q/3)$. To model the adiabatic transition of the lattice, we adopt a simple model in which $V(s)$ varies according to [1]

$$V(s) = \left[1 + \exp\left[\left(L_{1/2} - s\right)/L_{tr}\right]\right]^{-1} - \left[1 + \exp\left(L_{1/2}/L_{tr}\right)\right]^{-1}, \quad (2)$$

where $2L_{1/2}$ is the length of the transition section, and $L_{\rm tr}$ is the characteristic length scale for variation of $V(s)$.

The present approach for adiabatic formation of a beam quasi-equilibrium matched to a quadrupole lattice, can be generalized to the case of a periodic solenodial lattice. For the case of a solenoidal lattice, to maintain the average (smooth-focusing) effects of the total focusing field fixed, the transition of the applied lattice force is specified by

$$F_{sol} = -\left\{\left[1 - \left(1 - \bar{\kappa}_{sol}/\kappa_{sf}^{sol}\right)V^2(s)\right]\kappa_{sf}^{sol} + V(s)\,\delta\kappa_{sol}(s)\right\}\left(x\mathbf{e}_x + y\mathbf{e}_y\right), \quad (3)$$

where $\kappa_{\rm sol}(s)$ is the solenoidal lattice coupling coefficient,

$$\bar{\kappa}_{sol} = S^{-1}\int_{s_0}^{s_0+S} ds\,\kappa_{sol}(s), \quad (4)$$

and $\delta\kappa_{sol}(s) \equiv \kappa_{sol}(s) - \bar{\kappa}_{sol}$. For the choice of the solenoidal lattice model shown in Fig. 1 it is straightforward to demonstrate that $\kappa_{sf}^{sol} = \eta_s\hat{\kappa}_s + (1/12)\eta_s^2(1-\eta_s^2)\hat{\kappa}_s^2 S^2$.

A similar approach for formation of a quasi-equilibrium beam distribution matched to a periodic focusing solenoidal lattice by means of adiabatic turn-on of the oscillating focusing field has been previously reported in [3]. However, the choice of the applied lattice force transition, $F_{\rm sol,}(s)$, considered in [3] did not provide a constant average (smooth-focusing) value of the focusing force. Furthermore, small oscillations of the beam envelope with variations in the rms beam radius of the order of 1% were observed. In addition, δF simulations, rather than full PIC simulations, were performed in [3].

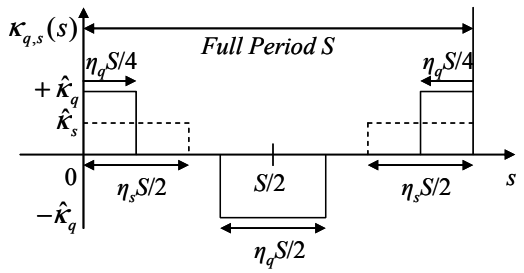

Fig. 1. Periodic-focusing coupling coefficients corresponding to a quadrupole lattice, $\kappa_q(s)$ (solid lines), and a solenoidal lattice, $\kappa_s(s)$ (dashed lines).

RESULTS OF THE NUMERICAL SIMULATIONS

The results of the numerical simulations for illustrative parameters corresponding to a moderate intensity beam with σ/σ_v=0.5, propagating through the quadrupole and solenoidal lattices shown in Fig. 1, are presented in Figs. 2-4. For the case of beam propagation through a quadrupole lattice, note that thermal equilibrium and waterbag equilibrium distributions have been used for the initial beam loading. To assure that matching is approximately maintained in the transition section, we choose $L_{1/2}$=5$L_{\rm tr}$, and take $L_{1/2}$=5$L_{\rm sf}$ for the quadrupole lattice case, and $L_{1/2}$=10$L_{\rm sf}$ for the solenoidal lattice case, where $L_{\rm sf}$ is the smooth-focusing period of the linear mismatched oscillations determined from [2] $L_{sf} = 2\pi S\Big/\sqrt{2\left(\sigma_v^{sf}\right)^2 + 2\left(\sigma^{sf}\right)^2}$, where σ_v^{sf} and σ^{sf} are the corresponding values of phase advances calculated within the smooth-focusing approximation. Figure 2 illustrates the discrete evolution of the normalized rms envelope x-dimension, $X_{rms} \equiv \langle x^2\rangle^{1/2}$, calculated at the end of each focusing cell where the beam x-envelope has a local maximum value, $X_{\rm max}$. Here, <···> denotes the statistical average over the beam distribution function; and $X_{\rm b0}$ used in the figures for normalization purposes corresponds to the initial (smooth-focusing) value of the rms envelope x-dimension. Along with the evolution of the beam parameters for the case of adiabatic turn-on of $V(s)$ shown by the solid curves, Fig. 2 also shows the evolution of beam parameters (dashed curves) for the case where the initial distribution is loaded instantaneously into a periodic lattice with $V(s)\equiv 1$. To load particles for this case, the smooth-focusing equilibrium distribution is first calculated, and then the positions and velocities of the beam particles are linearly scaled, providing the size and the slope of the beam envelope to be consistent with the matched solution to the envelope equations [1]. Note that the frames in (a) in Fig. 2 illustrate the initial evolution of the beam mismatch for the case of instantaneous loading, and the evolution near the exit of the transition section, $s \geq L_{1/2}$, for the case of adiabatic formation of a beam quasi-equilibrium.

It is evident from Fig. 2, for the case of adiabatic formation of the beam quasi-equilibrium, that the amplitude of the mismatch oscillations is reduced compared to the case of instantaneous loading of the beam distribution. Furthermore, note that the numerical scheme for instantaneous loading cannot intrinsically provide the detailed equilibrium, whereas for the case of adiabatic formation the beam mismatch can possibly be further suppressed if a finer grid and larger number of macroparticles are used in the simulations [1].

We now use the results of the numerical simulations for the case of adiabatic formation of the beam distribution to investigate properties of the beam density profile. Figures 3 and 4 show the evolution of the beam density projected along the x-direction for the cases of the quadrupole and solenoidal lattices, respectively. The profiles are calculated within the first lattice period after the beam leaves the transition section, i.e., $2L_{1/2} < s < 2L_{1/2} + S$. Note that plots in frames (a) and (c) show the normalized density profile $\tilde{n}_b(x,s) = \left[a(s)b(s)/R_{b0}^2\right]\left[n_b(x,y=0,s)/n_{b0}(r=0)\right]$ plotted versus the scaled coordinate $x/a(s)$. Here, $a(s) = \sqrt{2}X_{rms}(s)$, $b(s) = \sqrt{2}Y_{rms}(s)$, $R_{b0} = \sqrt{2}X_{b0}$, $n_b(x,y,s)$ is the beam density profile, and $n_{\rm b0}(r)$ is the initial density

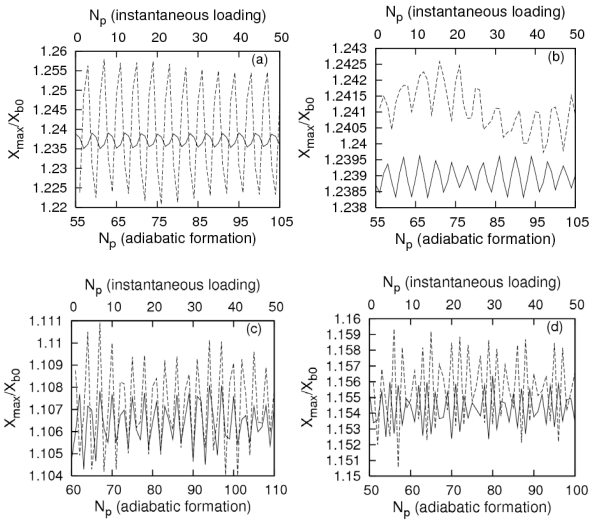

Fig.2. Plots of X_{max}/X_{b0} versus number of lattice periods, N_p. Frames (a) and (b) correspond to a quadrupole lattice with η_q=0.3, σ_v=57^0 (σ_v^{sf}=54^0), and the initial smooth-focusing beam equilibrium correspond to the thermal equilibrium and waterbag distributions, respectively. Frames (c) and (d) correspond to a solenoidal lattice with σ_v=84^0 (σ_v^{sf}=83^0) and σ_v=99^0 (σ_v^{sf}=97^0), respectively; here η_s=0.3 and the initial smooth-focusing beam equilibrium corresponds to a thermal equilibrium distribution. The solid curves correspond to adiabatic turn-on of the lattice, and the dashed curves correspond to the case of instantaneous beam loading.

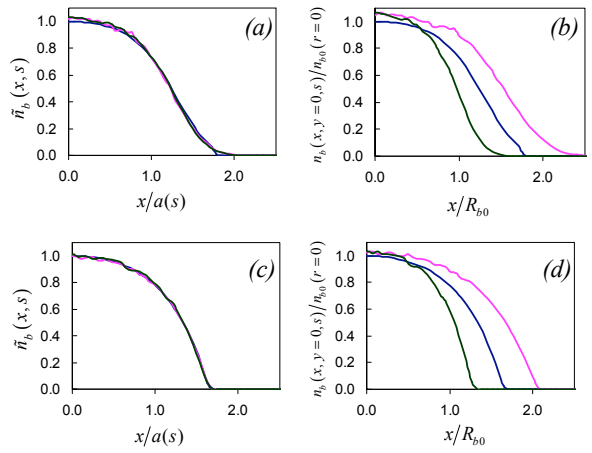

Fig. 3. Plots of the beam density profile for the case of a quasi-equilibrium beam distribution matched to a quadrupole lattice with η_q=0.3 and σ_v=57^0. Frames (a) and (b), and frames (c) and (d) correspond to initial thermal equilibrium and waterbag distributions, respectively. The density profiles correspond to: the initial smooth-focusing thermal equilibrium (blue curve); the maximum value of X_{rms} (pink curve); and the minimum value of X_{rms} (green curve).

profile corresponding to the azimuthally symmetric smooth-focusing equilibrium. It is readily seen that the evolution of the beam density profile is self-similar for any choice of periodic lattice structure and initial beam distribution. In addition, it is interesting to note that for the case of a solenoidal lattice the self-similarity feature is preserved to good accuracy even for σ_v=99^0, whereas for the case of a quadrupole lattice the self-similarity feature becomes less accurate for smaller values of vacuum phase advance (σ_v=87.5^0) [1].

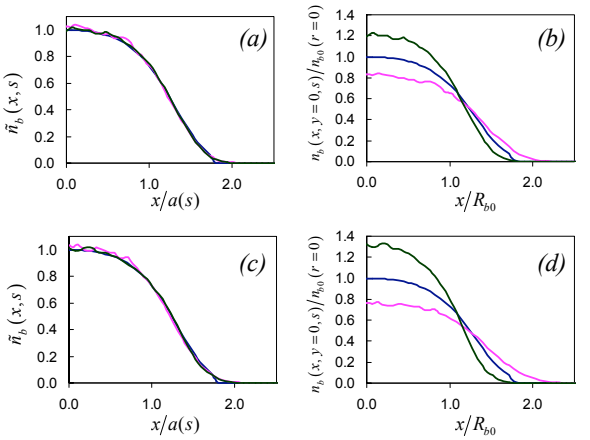

Fig. 4. Plots of the beam density profile for the case of a quasi-equilibrium beam distribution matched to a solenoidal lattice with η_s=0.3. Frames (a) and (b), and frames (c) and (d) correspond to σ_v=84^0 and σ_v=99^0, respectively. The initial smooth-focusing beam equilibrium corresponds to a thermal equilibrium distribution. The density profiles correspond to: the initial smooth-focusing thermal equilibrium (blue curve); the maximum value of X_{rms} (pink curve); and the minimum value of X_{rms} (green curve).

CONCLUSIONS

In this work we have continued the development of a numerical scheme for describing the quiescent loading of a quasi-equilibrium beam distribution matched to a periodic focusing lattice. The scheme was applied to both quadrupole and solenoidal lattices; and the thermal equilibrium and waterbag distributions have been considered for the initial beam equilibrium. Quiescent beam loading and self-similar evolution of the quasi-equilibrium matched beam density profile have been observed in numerical simulations for general choice of periodic lattice structure and initial beam distribution.

REFERENCES

[1] M.Dorf *et al.*, Phys. Rev. ST Accel. Beams, submitted for publication (2009).

[2] R. C. Davidson and H. Qin, *Physics of Intense Charged Particle Beams in High Energy Accelerators* (World Scientific, Singapore, 2001), and references therein.

[3] P. H. Stoltz *et al.*, Phys. Plasmas **6**, 298 (1999).